# Complementation *in trans* of altered thymocyte development in knock-in mice expressing mutant forms of SLP76

**Martha S. Jordan**[1,*], **Jennifer E. Smith**[1,*], **Jeremy C. Burns**[1], **Jessica-Elise T. Austin**[1], **Kim E. Nichols**[2], **Anna C. Aschenbrenner**[3], and **Gary A. Koretzky**[4]

1 *Cancer Biology, Abramson Family Cancer Research Institute, 427 BRBII/III, University of Pennsylvania School of Medicine, Philadelphia, PA, 19104*

2 *Pediatric Oncology, Wood, 4th floor, 3615 Civic Center Boulevard, Children's Hospital of Philadelphia, Philadelphia, Pennsylvania 19104, USA*

3 *University of Bonn, Bonn, Germany*

4 *Department of Pathology and Laboratory Medicine, 415 BRBII/III, University of Pennsylvania School of Medicine, Philadelphia, PA 19104*

## Summary

The adaptor protein SLP76 directs signaling downstream of the TCR and is essential for thymocyte development. SLP76 contains three tyrosines in its N-terminus that are critical for its function. To define the role of these residues in thymocyte development, we generated two lines of KI mice, one expressing a mutation in tyrosine 145 (Y145F) and a second harboring two point mutations at tyrosines 112 and 128 (Y112/128F). We show here that while thymocyte development requires both Y145 and Y112/128-generated signals, selection is more dependent upon Y145. While several proximal TCR signaling events were defective in both KI mice, phosphorylation of Vav1 and activation of Itk-dependent pathways were differentially affected by mutations at Y112/128 or Y145, respectively. Analysis of mice expressing one Y145F and one Y112/128F allele revealed that these mutants could complement one another *in trans*, demonstrating cooperativity between two or more SLP76 molecules.

## Introduction

During development, thymocytes must pass through several checkpoints. T cell progenitors enter the thymus as double negative [CD4$^-$CD8$^-$ (DN)] cells and progress in a TCR-independent manner through the DN1 (ckit$^+$CD25$^-$), DN2 (ckit$^+$CD25$^+$), and DN3 (ckit$^-$CD25$^+$) stages (Godfrey et al., 1993). At the DN3 stage, the pre-TCR is expressed, and signaling through this receptor is required for the transition to the final DN (DN4: ckit$^-$CD25$^-$) and double positive stages [CD4$^+$CD8$^+$ (DP)]. Only thymocytes with intact pre-TCR signaling pass this checkpoint, known as β-selection, and undergo proliferation and differentiation to become DP cells, at which time the mature αβ TCR is expressed (Michie and Zuniga-Pflucker, 2002). This TCR is tested during positive and negative selection, a second developmental stage in which intact TCR signaling is required (Miosge and Zamoyska, 2007). DP thymocytes capable of interacting with self-MHC ligands with sufficient avidity are

Corresponding author: Gary A. Koretzky, 215 746 5522 (p), 215 746 5525 (f), Koretzky@mail.med.upenn.edu.
*These authors contributed equally.

positively selected to mature into either CD4 single positive [CD4$^+$CD8$^-$ (CD4SP)] or CD8 single positive [CD4$^-$CD8$^+$ (CD8SP)] thymocytes, whereas those whose avidity is too strong are signaled to die by apoptosis. Collectively these processes generate a diverse T cell repertoire that is optimized for recognition of self-MHC complexed with foreign peptides.

Selection of T cells is governed by signals through the TCR/pre-TCR. Following TCR stimulation, the immunoreceptor tyrosine-based activation motifs (ITAMs) of the CD3 chains are phosphorylated by src protein tyrosine kinases (PTK), allowing for the recruitment of Syk family PTKs (Syk or ZAP-70), which subsequently phosphorylate key adaptor proteins. These adaptor proteins lack enzymatic activity but aid in the localization and activation of enzymes that are required for the generation of second messengers and signal propagation (Jordan et al., 2003).

The SH2 (Src homology 2) domain-containing leukocyte phosphoprotein of 76 kDa (SLP76) is one such adaptor protein that is critical for thymocyte development. Mice lacking SLP76 exhibit a complete developmental block at the DN3→DN4 transition, resulting in no DP or mature T cells (Clements et al., 1998; Pivniouk et al., 1998) or natural killer (NK) T cells (K. N. unpublished data). SLP76 has four functional domains: an N-terminal sterile α motif (SAM) domain, a C-terminal SH2 domain, a central proline-rich region, and an N-terminal acidic domain that contains three tyrosines at positions 112, 128, and 145 that are phosphorylated following TCR stimulation. Tyrosines at positions 112 and 128 are both part of a YESP motif and have been shown in Jurkat cells to bind to the guanine nucleotide exchange factor Vav1 and the adaptor protein Nck (Bubeck Wardenburg et al., 1998; Raab et al., 1997; Wu et al., 1996). Tyrosine 145 lies within a YEPP motif and has been implicated in binding IL-2 inducible T cell kinase (Itk) (Bunnell et al., 2000; Su et al., 1999). Through structure/function studies, the N-terminal tyrosines of SLP76 have been shown to be most critical for the function of this adaptor. Mutation of all three tyrosines in Jurkat cells leads to defective Ca$^{2+}$ release and MAPK activation (Musci et al., 1997; Yablonski et al., 2001). *In vivo*, transgenic expression of a Y112/128/145F (Y3F) SLP76 mutant on a SLP76-deficient background leads to DP but very few mature SP thymocytes and a 10-fold reduced thymus size (Kumar et al., 2002; Myung et al., 2001).

Given the central role of the SLP76 N-terminal tyrosines in the function of this adaptor, we recently undertook studies investigating their individual functions using the Jurkat model system (Jordan et al., 2006). These studies identified tyrosine 145, the proposed site for Itk binding, as the most important individual tyrosine for mediating TCR signal transduction. To determine the impact of this tyrosine *in vivo*, we have generated KI mice that contain a tyrosine to phenylalanine (Y→F) mutation at position 145 of SLP76. A second, complementary mouse containing Y→F mutations at the remaining two tyrosines residues (112 and 128) was also generated. Both KI mice demonstrate defective positive and negative selection, NKT cell development, T cell:APC conjugate formation, and activation of several proximal signaling molecules. However, these mutants show differential activation of Vav1 and Itk-dependent pathways. Additionally, we found that when these two mutants are coexpressed they are able to rescue one another *in trans*.

## Results

### Generation of SLP76 KI mice

We established previously that there is a functional hierarchy of the three N-terminal tyrosines of SLP76, with the tyrosine at position 145 being more important for signaling in Jurkat cells than single mutations at either of the remaining two tyrosines (Y112 and Y128) (Jordan et al., 2006). To determine how mutation at Y145 affects thymocyte development, we generated mice that carry a single nucleotide point mutation (an A→T substitution resulting in altering a

tyrosine to phenylalanine) at this position. As a complementary mutation, we generated a mouse with tyrosine to phenylalanine substitutions at the other N-terminal sites Y112 and Y128 (Figure S1 A, B). SLP76 protein expression was not altered as a result of targeting exon 7 as measured by flow cytometry (Figure S1 C). Both Y145F and Y112/128F mice were generated at Mendelian ratios with no evidence of the perinatal lethality (Clements et al., 1998) or the vascular defect (Abtahian et al., 2003) that is observed in SLP76-deficient mice.

## Thymocyte development in SLP76 KI mice

Y145F and Y112/128F KI mice are both capable of generating mature SP thymocytes (Figure 1A). While there are mild decreases in total thymic cellularity and subtle differences in the percentage of thymocytes within the DN, DP, CD4SP, and CD8SP stages when compared to wild-type (WT) mice, there are significant differences in the CD4SP:CD8SP ratio between WT and both KI lineages (Table S1). Further analysis of the DN stages of development revealed that Y145F and Y112/128F mice have a partial defect in transitioning from DN3 to DN4 (Figure 1A), the stage at which SLP76-deficient mice display a complete block (Clements et al., 1998).

In addition to conventional αβ T cells, the thymus also generates natural NKT cells. Most NKT cells express an invariant TCRα chain (Vα14-Jα18) in combination with particular Vβ chains and can be identified by positive staining with glycolipid-antigen loaded CD1d tetramers. While the early stages of NKT cell development proceed in large part in the thymus, final maturation may occur in the periphery (Godfrey and Berzins, 2007). Thus, using tetramers loaded with an analog of α-galactosyl-ceramide (PBS57) to identify NKT cells and CD44 and NK1.1, markers of early and late NKT cell maturation, respectively, we analyzed NKT cell development in WT and SLP76 KI mice. The frequency and absolute number of thymic NKT cells were decreased in Y112/128F mice and to a greater extent in Y145F mice (Figure 1B, C). While the percent of CD44$^+$ cells was only slightly decreased among KI versus WT NKT cells, NK1.1 expression was markedly diminished. This defect was even more pronounced in the spleen and liver (Figure 1C). Thus, in addition to defects in αβ T cell development, NKT cell development in SLP76 KI mice is substantially altered.

## Defective selection of SLP76 KI thymocytes

Despite the relatively normal thymic profile of Y145F and Y112/128F mice, thymocyte development is altered in these mice, as evidenced by their decreased expression of key surface markers. As thymocytes transition from DN to DP, they upregulate CD5, CD2, and CD3 expression in response to pre-TCR and TCR signaling (Azzam et al., 1998; Duplay et al., 1989). While CD3 levels are similar between WT and KI mice at this stage, upregulation of CD5 and CD2 fails to occur in both Y145F and Y112/128F thymocytes, indicating that signaling from the pre-TCR is defective (Figure 2A, data not shown). Progression to the SP stage is accompanied by further increases in these molecules (Duplay et al., 1989; Tarakhovsky et al., 1995). Despite their severe defect in CD5 and CD2 expression at the DP stage, SP thymocytes from Y112/128F mice have normal CD5, CD2, and CD3 expression, and Y145F SP thymocytes have only slightly reduced expression of the molecules (Figure 2A and data not shown). Since CD5 expression correlates directly with TCR affinity, the shift in CD5 levels seen at the DP stage in the KI mice suggests that TCR signaling is dampened (Azzam et al., 1998).

To investigate the ability of KI thymocytes to undergo negative selection, we assessed whether KI DP thymocytes could upregulate the orphan nuclear receptor Nur77 following *in vitro* stimulation. Nur77 is induced in DP thymocytes subjected to apoptotic signals *in vitro* (TCR/ CD28) and in response to negatively selecting ligands *in vivo* (Cho et al., 2003; Cunningham et al., 2006). Nur77 was robustly induced in WT DP thymocytes after a 2h stimulation *in*

*vitro* but only weakly upregulated in Y145F and Y112/128F DP thymocytes (Figure 2B). Stimulation of KI thymocytes also resulted in diminished down modulation, or "dulling", of CD4 and CD8 on DP thymocytes following TCR/CD28 stimulation as compared to WT thymocytes (Figure 2C). DP dulling occurs on apoptotic thymocytes (Kishimoto et al., 1995) and on thymocytes transitioning to the SP stage (McGargill and Hogquist, 1999) and has been used as an indicator of both negative and positive selection events. Thus, the reduction of DP dulling in KI thymocytes is consistent with altered thymocyte signaling and possible defects in selection.

To more directly address the efficiency of negative selection in SLP76 KI mice, deletion of T cells bearing Vβ chains susceptible to superantigen engagement was assessed. Vβ11[+] and Vβ12[+] thymocytes are deleted in I-E[d+] mice expressing MMTV-8 and MMTV-9 proviral gene products. Therefore, C57BL/6×129 KI mice were backcrossed to Balb/c mice and screened for expression of MHC[d] (C57BL/6, Sv129, and Balb/c mice all express MMTV-8 and -9) (Peterson et al., 1985; Salinas et al., 1987). In WT mice and Y112/128F heterozygous littermates, Vβ11[+] and Vβ12[+] thymocytes underwent superantigen-induced deletion from the DP to CD4SP stage (Figure 2D). In contrast, Y145F mice failed to delete Vβ11[+] and only partially deleted Vβ12[+] thymocytes. Y112/128F thymocytes also showed defects in superantigen-mediated deletion but to a lesser extent compared to Y145F thymocytes. Thymocytes expressing non-susceptible Vβ chains (Vβ8 and Vβ6) were found at expected frequencies in WT and KI mice (Figure 2D and data not shown).

Negative selection of MHC class I restricted thymocytes through peptide:MHC interactions was assessed in male mice expressing a TCR transgene specific for the male HY antigen (Teh et al., 1989). Thymocyte development in WT male mice expressing the HY TCR transgene is arrested at the DN stage (Takahama et al., 1992). This block was substantially alleviated in Y112/128F and Y145F mice allowing for maturation to the DP stage and, in the case of Y145F mice, development into CD8SP cells (Figure 2E and S2). The increased proportion of DP and CD8SP populations in Y145F mice was accompanied by a three-fold increase in thymic size compared to WT male mice (Figure S2).

Positive selection in SLP76 KI mice was determined by their ability to select the MHC class II-restricted AND TCR (Kaye et al., 1989). In WT AND[+] mice, CD4SP cells represent, on average, 37% of the thymus and nearly all express high levels of the transgenic TCR (Figure 3A). This level was reduced to 4.8% and 2.3% in Y112/128F and Y145F mice, respectively. Although both KI strains demonstrated significant defects in positive selection, these defects were more profound in the Y145F lineage as evidenced by an approximate 75% loss of Vα11/ Vβ3 transgenic TCR expression among CD4SP thymocytes as compared to WT CD4SP, a reduction far greater than that observed in Y112/128F mice. Co-staining with a pan anti-TCRβ reagent revealed that the low Vβ3 expression in Y145F mice was not due to the use of endogenous Vβ chains but rather to overall reduced TCR expression (data not shown). Since immature thymocytes express low levels of TCRβ, it was possible that the CD4SP thymocytes present in the Y145F KI were immature. To determine whether this was the case, we analyzed the CD4SP thymocytes for their expression of HSA, a marker that is high on immature and low on mature thymocytes (Crispe and Bevan, 1987). Despite their low level of TCRβ expression, CD4SP thymocytes from Y145F mice were HSA[low], indicating that these cells were indeed mature (data not shown).

Intact thymocyte selection correlates with the ability of DP thymocytes to form conjugates with antigen-presenting cells (Ardouin et al., 2003; Richie et al., 2002; Wu et al., 2006). To examine this function in SLP76 KI mice, thymocytes from WT and KI mice on the AND transgenic background were incubated with pigeon cytochrome c (PCC) peptide (the antigen recognized by AND transgenic T cells) pulsed B cells. Since the expression level of the AND

transgenic TCR is lower on KI compared to WT thymocytes, we focused our analysis on cells expressing the same level of Vα11. We observed that DP thymocytes from both KI mice formed fewer conjugates as compared to WT thymocytes (Figure 3B). Consistent with decreased TCR-induced conjugate formation, Y112/128F and Y145F thymocytes were impaired in TCR-induced actin polymerization (Figure 3C), a process required for conjugate formation (Huang and Burkhardt, 2007). Thus, the defects seen in both positive and negative selection in Y145F and Y112/128F mice may be due in part to defective interactions with thymic antigen presenting cells.

## Proximal TCR signaling is defective in SLP76 KI mice

Mutation of tyrosine residues within the N-terminus of SLP76 is predicted to lead to loss of SLP76 phosphorylation. Indeed, mutation of Y112 and Y128 ablated nearly all detectable SLP76 phosphorylation (Figure 4A); mutation of Y145, however, resulted in little diminishment of total phosphorylation. These data are consistent with our previous studies in Jurkat cells in which Y145 was shown to be phosphorylated, but optimal phosphorylation occurred only when Y112 or Y128 were intact (Jordan et al., 2006). It is unclear why the Y112/128F KI does not have a more severe phenotype than the Y145F mouse. It is possible that little phosphorylation is required for Y145 function or that Y145 supports phosphorylation-independent functions. SLP76 phosphorylation was also analyzed using a pY128 specific antibody. Stimulated Y112/128F thymocytes failed to react with the pY128 antibody, whereas WT and Y145F thymocytes were capable of phosphorylating this site (Figure 4B). Global loss of tyrosine phosphorylation was not observed in either KI mutant, rather loss of phosphorylation of a 95kDa species was noted in Y112/128F thymocytes (Figure 4C). To probe whether events upstream of SLP76 were intact, we assessed TCR-induced phosphorylation of tyrosine 191 on LAT and found this process to be normal in both mutants (Figure 4B).

To address the biochemical mechanism(s) underlying the selection defects observed in SLP76 KI mice, we analyzed PLCγ1 phosphorylation, $Ca^{2+}$ flux, and ERK phosphorylation following TCR stimulation. Using unfractionated thymocytes, we observed that PLCγ1 and ERK phosphorylation were markedly diminished in both KI mice following TCR stimulation (Figure 4D, E). Similar defects in ERK phosphorylation were noted in purified DP thymocytes after TCR/CD4 co-crosslinking (Figure S3) and $Ca^{2+}$ flux was diminished in both DP and CD4SP thymocytes (Figure 4F). Tyrosines 112 and 128 of SLP76 have been shown in Jurkat cells to be the sites responsible for inducible Vav1 association (Raab et al., 1997; Wu et al., 1996). Based on this knowledge, we reasoned that in Y112/128F mice SLP76/Vav1 binding would be abolished. Instead, we found that this association in Y112/128F thymocytes was preserved (Figure S4 A). Moreover, we did not detect inducible association of Vav1 with SLP76 in WT mice, despite robust inducible SLP76 phosphorylation. However, we did observe that there was a near complete loss of TCR-induced Vav1 phosphorylation in Y112/128F thymocytes (Figure 5A), consistent with the loss of a phosphorylated species at 95kDa as seen by anti-phosphotyrosine (Figure 4C). Importantly, there was only a mild decrease in Vav1 phosphorylation in Y145F thymocytes.

Similar to the preserved SLP76/Vav1 binding in Y112/128F thymocytes, mutation of Y145 (the proposed Itk phosphorylation-dependent binding site on SLP76) did not result in loss of SLP76/Itk association (Figure S4 B). In Jurkat cells it was recently shown that the N-terminal tyrosines of SLP76 are responsible for Itk phosphorylation and activation and that catalytically active Itk was preferentially associated with SLP76 (Bogin et al., 2007). Thus, tyrosine 145 may be responsible for activating Itk. If this scenario is correct, then the phenotype of Y145F mice would be similar to that of Itk-deficient mice. Itk-deficient T cells have been reported to have decreased ERK and PLCγ1 phosphorylation and diminished $Ca^{2+}$ flux following TCR stimulation (Liu et al., 1998; Schaeffer et al., 1999). Both Y145F and Y112/128F mice share

these characteristics (Figure 4D–F). Recently, CD8SP thymocytes from Itk-deficient mice were shown to express high levels of CD122 and CD44 and low HSA levels (Atherly et al., 2006; Broussard et al., 2006). Significantly, this cell surface phenotype was seen in CD8SP thymocytes from Y145F mice (Figure 5B). Expression of these markers was variably upregulated on Y112/128F CD8SP thymocytes (and peripheral CD8^{+} T cells) but never to levels seen in Y145F mice (data not shown). Moreover, purified CD69^{+} CD8SP thymocytes from Itk-deficient mice, but not WT mice, were shown to express high levels of eomesodermin mRNA (Atherly et al., 2006). To determine whether altered eomesodermin regulation was also shared by Y145F and/or Y112/128F thymocytes, we purified CD8SP CD69^{+} (a marker of recently selected cells) thymocytes and performed real-time PCR. Eomesodermin message levels were ~65-fold greater in Y145F than WT or Y112/128F purified cells (Figure 5C). Taken together, these data reveal that while Y112/128 and Y145 contribute similarly to TCR induced $Ca^{2+}$ flux and phosphorylation of PLCγ1 and ERK, Y112/128 and Y145 are differentially required for Vav1 phosphorylation and phenotypes associated with Itk deficiency, respectively despite the preserved association of mutated SLP76 with these binding partners.

### Complementation of SLP76 mutations in vivo

Since Y112/128F and Y145F thymocytes show distinct differences in their abilities to support Vav1 and Itk function, we asked whether co-expression of these mutants could complement one another functionally (Figure 6A). To this end, we generated "double mutant" mice bearing one Y112/128F allele and one Y145F allele. Double mutant mice were compared to WT and SLP76 single KI mice in multiple phenotypic and functional assays. In all cases, responses of the double mutant cells were greater than either single KI mouse and in some cases identical to that observed for WT mice. For example, the CD5/CD3 thymic profile of Y112/128F and Y145F mice was strikingly defective; however, co-expression of the two mutants resulted in nearly normal CD5/CD3 expression (Figure 6B). Functionally, the ability of mutant thymocytes to upregulate Nur77, to phosphorylate PLCγ1 and ERK, and to flux $Ca^{2+}$ was similar to or only slightly reduced from that observed in WT thymocytes (Figure 6C–E). We did not observe a dominant negative effect of expressing the Y112/128F and Y145F mutations simultaneously, inasmuch as Vav1 phosphorylation, which was nearly normal in Y145F mice but defective in Y112/128F mice, was normal in the double mutant (data not shown). Similarly, double mutant CD8SP thymocytes were not CD122^{+}HSA^{low}, a phenotype of Y145F but not Y112/128F mice (Figure 6F). Thus, based on both phenotypic and functional data, these two distinct mutants of SLP76 can complement each other *in trans* in developing thymocytes.

## Discussion

In this study we have modified SLP76, a key signaling molecule downstream of the TCR, to dissect how it supports signaling pathways important for thymocyte development and to understand how it coordinates formation of a signaling complex. Expression of SLP76 harboring mutations at tyrosines 112 and 128 as a pair or 145 independently resulted in multiple defects in thymocyte development. Our data show that these tyrosine "units" are important for efficient pre-T cell signaling, NKT cell development, and proper αβ T cell selection. Additionally, we provide evidence that lack of a functional tyrosine at position 145 results in the development of CD8^{+} cells that possess characteristics of innate-like lymphocytes.

Both Y112/128F and Y145F KI mice have an increase in the percentage of DN3 thymocytes, indicative of defective pre-TCR signaling. There were only minor diminishments in the absolute number of DP thymocytes from KI compared to WT thymocytes indicating that pre-TCR signaling from KI mice could support, in large part, DP differentiation. However, failure to upregulate CD5 at this stage points to defective pre-TCR signaling, inasmuch as TCRα^{−/−} mice, which must rely on the pre-TCRα chain for signaling, are fully capable of CD5

upregulation from the DN→DP stage (Azzam et al., 1998; Schaeffer et al., 2000; Turner et al., 1997). Thus, early signals from the pre-TCR are dependent upon tyrosines 112/128 and 145.

Once at the DP stage, thymocytes can either be selected into the classical αβ T cell pool or into an alternative lineage, such as the NKT lineage. SLP76 KI mice generate NKT cells that express near WT levels of CD44 (Figure 1C) and HSA (data not shown), indicating normal progression through the early stages of NKT cell ontogeny. In contrast, upregulation of NK1.1 was diminished, most notably in the periphery. Failure to express NK1.1 was most marked in Y145F mice and is similar to that observed on Itk-deficient NKT cells (Gadue and Stein, 2002). From these data we speculate that Y145-dependent activation of Itk is important for progression through the late stages of NKT cell development where cells acquire expression of NK1.1.

Since SLP76-deficient thymocytes do not develop past the DN3 stage, the specific role of SLP76 in positive and negative selection has been difficult to study. Using directed mutagenesis of the tyrosines of SLP76, we show here that point mutations in this molecule can result in dramatic defects in positive and negative selection. Defective negative selection of MHC class I- and class II-restricted thymocytes in SLP76 KI mice was demonstrated by failure to efficiently negatively select HY-reactive thymocytes in male mice or to delete SP thymocytes expressing Vβ11 and Vβ12 TCR chains in response to endogenous superantigens. Both of these models point to Y145 as being more critical for effective negative selection. In fact, in HY Y145F males, there was an increase in thymus size compared to WT HY males and the emergence of CD8SP thymocytes that express relatively high levels of the HY clonotype (data not shown). Thus it appears that in Y145F male mice, the HY antigen is driving positive selection of HY clonotype[+] thymocytes. In contrast to the *in vivo* models, *in vitro* upregulation of Nur77 following anti-CD3/CD28 stimulation was similarly defective in both KI lineages. These data underscore that while Nur77 expression in DP thymocytes, as measured under these experimental conditions, is a marker of cells fated to undergo apoptosis, it alone may not be sufficient to induce deletion and represents only one of many pro-apoptotic proteins induced during negative selection. Experiments are underway to identify other pathways known to be important for negative selection in an effort to identify targets that are differentially activated in Y112/128F versus Y145F thymocytes.

Positive and negative selection are dependent upon calcium signals and the location, magnitude, and duration of Ras/MAPK signaling (Cante-Barrett et al., 2006; Daniels et al., 2006; Mariathasan et al., 2001; McNeil et al., 2005; Neilson et al., 2004). The ability of thymocytes to form conjugates with APCs has also been associated with proper thymocyte selection. SLP76 KI mutants are defective in all of these functions as are mice deficient in Itk and Vav1 (Costello et al., 1999; Krawczyk et al., 2002; Labno et al., 2003; Schaeffer et al., 1999).

Y112/128F mice have a near complete loss of Vav1 phosphorylation following TCR stimulation. Y145F thymocytes, however, had only subtle defects in Vav1 phosphorylation, yet the phenotype of these cells was strikingly similar to that of Itk-deficient mice. In fact, side-by-side comparisons of the two revealed many similarities. One characteristic shared between Itk-deficient mice and Y145F mice was the development of CD8 innate-like lymphocytes. This thymocyte subset was recently found to preferentially develop (compared to that of conventional CD8^{+} αβ T cells) in Itk-deficient mice (Atherly et al., 2006; Broussard et al., 2006). The innate-like CD8SP cells present in Itk-deficient mice are CD44^{hi}, CD122^{hi}, contain elevated levels of eomesodermin message, and produce high amounts of IFN-γ upon direct *ex vivo* stimulation. The CD8SP thymocytes from Y145F mice are also CD44^{hi}, CD122^{hi}, contain high eomesodermin message (Figure 5C), and produce IFN-γ directly *ex vivo* (data not shown). Thus, in addition to the similarities between Itk-deficient and Y145F mice in terms of selection and signaling, Y145F mice also generate innate-like CD8^{+} cells. Although further analyses

may reveal differences between Y145F and Itk-deficient mice, it is striking that a single point mutation in SLP76 results in a phenotype that so closely mimics that of Itk deficiency. Our data suggest that many of the functions of Itk may be largely dependent upon SLP76. Tyrosines 112 and 128 may contribute to Itk activation as well, since these tyrosines are required for Vav1 phosphorylation and Vav1 is a known regulator of Itk (Reynolds et al., 2002). This possibility may contribute to why $CD8^+CD44^+$ cells are occasionally seen in Y112/128F mice.

A simple model for how the N-terminal tyrosines of SLP76 support thymocyte signaling is that each tyrosine binds its respective binding partner following tyrosine phosphorylation and allows for activation of associated enzymes. Indeed we predicted, based on previous studies in Jurkat cells performed by our laboratory and others, that mutation of tyrosines at positions 112 and 128 or 145 would abolish the SLP76/Vav1 or SLP76/Itk associations, respectively. As noted, we have not seen a marked TCR-inducible association between SLP76 and these two proteins in primary murine T cells. These constitutive associations may reflect an assembled signaling complex that is necessary to support tonic TCR signals *in vivo*, and we speculate that although tyrosines 112, 128, and 145 are important for binding Itk and Vav1, their contributions are not appreciated in primary T cells due to tertiary protein/protein interactions. Consistent with these data, we do not see appreciable inducible binding of Vav1 and Itk even in WT thymocytes after TCR stimulation although there is robust inducible SLP76 phosphorylation (Figure S4).

Although the molecular interactions responsible for the pattern of protein/protein interactions we observe in WT and KI mice are unclear, the selective loss of Vav1 phosphorylation in Y112/128F thymocytes and the developmental similarities between Itk-deficient and Y145F thymocytes suggest that the activity of these proteins are regulated by Y112/128 and Y145, respectively. According to this model, Itk in Y145F mice could associate with SLP76 via tertiary interactions or perhaps directly through the SH3 domain of Itk, as has been reported (Bunnell et al., 2000). However, Itk function would not be induced due to lack of the tyrosine phosphorylation site at position 145 of SLP76. Indeed, the SH2 domain of Itk has been proposed to require interaction with a phosphotyrosine in order for it to acquire kinase activity (Pletneva et al., 2006). This failure to activate Itk would result in diminished PLCγ1 phosphorylation and $Ca^{2+}$ flux (Liu et al., 1998). Similarly, Vav1 may associate with a SLP76 complex via indirect interactions, however in the absence of Y112/128 Vav1 fails to become phosphorylated. Although associated with SLP76, loss of phosphorylation at Y112/128 may prevent a Vav1/SLP76 interaction that is required for a conformational change in Vav1 that is necessary for access by its kinase. Lack of Vav1 phosphorylation may impact PLCγ1 activation by affecting the Vav1-regulated, PI3K-dependent activation of Itk or the interaction between PLCγ1 and SLP76 (Reynolds et al., 2002). Determining if tyrosines 112 and 128 regulate GEF activity may help distinguish between these two possibilities. Although JNK (c-Jun amino-terminal kinase) is a target of Vav1 GEF activity in cell lines, we did not note a substantial decrease in JNK phosphorylation (Figure S5), consistent with a prior study that reported normal JNK phosphorylation in Vav1-/-thymocytes (Fischer et al., 1998). Analysis of other Vav1 GEF targets and direct assessment of both Vav1 and Itk enzymatic activity are currently underway.

A great deal is known about the signaling pathways supported by individual adaptor proteins. Much less is known about how domains within a protein work together to support *in vivo* functions. We addressed this question regarding the three N-terminal tyrosines of SLP76 by attempting to genetically complement one mutation with the other. Using phenotypic, functional, and biochemical read-outs, double mutant KI mice partially and in some instances fully rescue the single mutant phenotypes. Our data clearly demonstrate that the binding partners of SLP76 are not required to assemble on a single SLP76 molecule and that the cooperativity between mutant SLP76 molecules occurs early following TCR stimulation, as $Ca^{2+}$ flux and activation of proximal signaling molecules such as PLCγ1 and ERK are restored

in double mutant mice. Proteins that inducibly associate with SLP76 have been shown to oligomerize following TCR stimulation. For example, Grb2 induces the oligomerization of LAT after TCR ligation (Houtman et al., 2006). SLP76 binds inducibly to LAT via GADS. Thus, it is likely that the complex that forms subsequent to TCR ligation includes at least two SLP76 molecules. The partial rescue seen in some assays leads us to speculate that the *trans* complex is not as stable as a *cis* complex or that recruitment of other key proteins to the signaling complex may be inefficient. This idea is consistent with data from Itk knockdown Jurkat cells and Vav1-deficient thymocytes, in which the absence of Itk or Vav1 resulted in the destabilization of the SLP76/Vav1 and SLP76/PLCγ1 associations, respectively (Dombroski et al., 2005; Reynolds et al., 2002).

To our knowledge, these data describe the first example of *in vivo trans*-complementation by a lymphocyte adaptor protein. In fact, the ability of the Y112/128F and Y145F mutations to complement one another *in trans* is in contrast to the lack of complementation seen between two mutations in the SLP76 homolog, BLNK (B cell Linker protein), in BLNK deficient DT40 cells (Chiu et al., 2002). While these results may reflect differences between primary T cells and B cell lines, they may be a consequence of broader signaling differences downstream of various ITAM bearing receptors. In T cells, SLP76 is organized into a large multimolecular signalasome influenced by the complement of molecules involved in TCR signaling. For example, TCR signal transduction is supported by ten ITAMs, utilizes the Syk kinase ZAP70, and is absolutely dependent upon LAT (a protein known to oligomerize) for signal propagation (Zhang et al., 1999). Conversely, B cell signaling utilizes only two ITAMs, signals through Syk, and is independent of LAT. Since SLP76 is not expressed in mature B cells, a direct comparison of the ability of the Y112/128F and Y145F mutations to complement one another in B and T cells is not possible. However, SLP76 is expressed in platelets, neutrophils, and mast cells. All of these cell types depend upon SLP76 for proper ITAM mediated signaling. Comparisons in the ability of the tyrosine mutations described herein to complement one another *in trans* in a variety of cell types are currently underway and will likely provide unique insight into how a single adaptor functions in distinct lineages.

## Experimental Procedures

### Mice

KI mice were backcrossed to C57BL/6 mice 2-5 times. Itk-deficient thymi were the kind gift of Pamela Schwartzberg. All animal experiments were preformed in accordance with University guidelines.

### Flow cytometry

Thymocytes were harvested, washed, and stained with antibodies in FACS buffer (PBS containing 2% FBS and 0.002% azide) for 30 min. Samples were collected on a FACSCalibur (BD Biosciences), and analysis was performed using FlowJo software (Tree Star). Fractionated thymic populations were sorted on a BD FACSAria. Liver lymphocytes were isolated as previously described (Watanabe et al., 1992). Antibodies for flow cytometry were purchased from BD Pharmingen: anti-CD4 PE or PerCpCy5.5, anti-CD8 allophycocyanin or FITC, anti-CD3 PE, anti-Vβ3 FITC, anti-Vα11 PE, anti-Rat Ig FITC, anti-Nur77, anti-CD122 PE, anti-CD44 FITC, anti-Vβ6 FITC, anti-Vβ8 FITC, anti-Vβ11 PE, anti-Vβ12 biotin followed by streptavidin PE, anti-B220 allophycocyanin or FITC, anti-ckit allophycocyanin, anti-CD25 PerCpCy5.5, anti-Thy1.2 allophycocyanin, anti-ckit PE, anti-CD24 FITC, anti-TCRβ allophycocyanin, PE or FITC, anti-CD5 FITC, anti-CD2 PE, PBS57-CD1d tetramer-allophycocyanin (NIH tetramer Core Facility), and NK1.1 PerCp. FITC conjugated lineage markers were as follows: anti-CD8, anti-γδ, anti-DX-5, anti-B220, anti-NK1.1, anti-Mac1, and anti-Gr1. Phalloidin-488 was purchased from Molecular Probes.

### Nur77 upregulation and coreceptor downregulation

Freshly isolated thymocytes were plated ($1\times10^6$ cells) onto a 24-well dish coated with anti-CD3 (10μg/ml) ± anti-CD28 (50μg/ml). Cells were cultured at 37°C for 2h (Nur77) or 5h (coreceptor downregulation). For coreceptor downregulation, cells were stained with anti-CD4 and anti-CD8 antibodies and collected on a FACSCalibur. For Nur77 analysis thymocytes were harvested and fixed (1% PFA for 10min at room temperature) and permeabilized in cold methanol for 30min or overnight. Cells were rehydrated in PBS and stained with anti-CD4, anti-CD8, anti-Nur77 followed by anti-Rat Ig FITC antibodies.

### Vβ deletion

KI mice and heterozygous littermates were backcrossed to Balb/c mice for three generations. Several mice used in these studies harbored an irrelevant hemagglutinin transgene that was carried through the backcrosses for other purposes. WT mice were backcrossed 3-10 ten times. The percent DP and CD4SP thymocytes expressing Vβ6, 8, 11, and 12 was determined by flow cytometry.

### Conjugate formation

B cells (LK35.2) were incubated for 1h at 37°C with anti-B220 with or without 10 μM PCC. Cells were washed and resuspended at $1\times10^7$ cells/ml. Splenocytes were stained with anti-CD4, anti-CD8 and anti-Vα11 antibodies, washed and resuspended to $1\times10^7$ cells/ml. Cells were mixed at a 1:1 ratio (100μl of each), spun in a Beckman tabletop centrifuge for 2min at 1200 rpm at 4°C, then placed in a 37°C water bath for 12min. Cold media containing 0.02% azide was added to stop conjugate formation. Cells were gently mixed by pipetting three times before collection on a BD FACSCalibur.

### F-actin staining

Thymocytes were rested in IMDM containing 1% BSA for 45 min then stained with 2μg/ml anti-CD3 (2C11; Pharmingen) on ice for 20 min. Cells were washed and resuspended in warm PBS/1% BSA for 5 min after which time cells were removed for the unstimulated time point. Anti-CD3 was cross-linked with goat-anti-hamster (1μg/ml) for various time points. Cells were fixed for 10 min in 1% paraformaldehyde, washed, permeabilized in 1% Triton/PBS for 5 min, washed and stained with phalloidin, anti-CD4 and anti-CD8.

### Immunoprecipitations and Western blots

Thymocytes were rested at 37°C in IMDM (no serum) for 30 min, after which time they were stimulated with 5μg/ml of anti-CD3 (500A2; Pharmingen) at 37°C for various amounts of time. Ice-cold PBS was added to stop the stimulations. Cells were pelleted and lysed: 1% NP-40, 150mM NaCl, 50mM Tris HCl (pH 7.5), 1mM Na$_3$VO$_4$, 5mM NaF, 1mM PMSF, Protease Inhibitor Cocktail (Sigma), 5mM Na pyrophosphate. For immunoprecipitations, lysates were incubated, rotating at 4°, with either anti-SLP-76 (eBioscience) or anti-Vav1 (Cell Signaling) for 2 to 3 h after which 50μl of anti-mouse or anti-rabbit Trueblot beads (eBioscience) were added and the mixture was incubated for an additional hour. Beads were washed 4 times with lysis buffer and resuspended in 50μl 2X Laemmli's reducing buffer (Boston Bioproducts), boiled, and analyzed by Western blot. Western blots were probed with the following antibodies: 4G10 anti-phospho-tyrosine (Upstate), phospho-PLCγ-1 (Tyr783), PLCγ-1, phospho-p44/42 MAPK (Thr202/tyr202), phospho-LAT (Tyr191) (all from Cell Signaling), and ERK2 (Santa Cruz), phospho-SLP-76 (Tyr128) (BD biosciences).

## Ca²⁺ flux

Thymocytes were loaded in RPMI containing 1% serum with 2 μg/ml of Indo-1 (Molecular Probes) in the presence of 4mM probenecid at 30°C for 30 min. Cells were concurrently stained with biotinylated-2C11, biotinylated anti-CD4 (clone RMA-4), anti-CD4 PE (clone GK1.5), and anti-CD8 FITC. Washed cells were resuspended in serum-free RPMI, warmed to 37°C, and baseline $Ca^{2+}$ levels were measured for 30s before addition of streptavidin (12.5 μg/ml) (Molecular Probes). $Ca^{2+}$ release was measured by a change in Indo-1 fluorescence, represented by the ratio of bound/unbound Indo-1. An LSR Bench top Flow Cytometer (BD Biosciences) was used for data collection, and FlowJo software (Tree Star) was used for analysis.

**Real-time RT-PCR—**CD4SP CD69⁺ and CD8SP CD69⁺ thymocytes were purified by FACS using anti-CD8 FITC, anti-CD4-allophycocyanin, and anti-CD69-PE. Thymocytes were washed and lysed with Trizol Reagent (Invitrogen). RNA was isolated using RNeasy kit according to the manufacturer's protocol (Qiagen). cDNA was made using Super Script III First Strand kit (Invitrogen). RT-PCR was performed using eomesodermin or GADPH primer/ probe mix from Applied Biosystems. Reactions were performed on a 7500 Fast Real-Time PCR System using FastTaq Master Mix (Applied Biosystems). For analysis, samples were normalized to GAPDH levels and then set relative to normalized CD4SP CD69⁺ eomesodermin message levels (relative quantity, RQ). Calculations were performed using Applied Biosystems software. Error bars represent the maximum and minimum possible RQ values. All samples were performed in triplicate.

## Supplementary Material

Refer to Web version on PubMed Central for supplementary material.

## References

Abtahian F, Guerriero A, Sebzda E, Lu MM, Zhou R, Mocsai A, Myers EE, Huang B, Jackson DG, Ferrari VA, et al. Regulation of blood and lymphatic vascular separation by signaling proteins SLP-76 and Syk. Science 2003;299:247–251. [PubMed: 12522250]

Ardouin L, Bracke M, Mathiot A, Pagakis SN, Norton T, Hogg N, Tybulewicz VL. Vav1 transduces TCR signals required for LFA-1 function and cell polarization at the immunological synapse. Eur J Immunol 2003;33:790–797. [PubMed: 12616499]

Atherly LO, Lucas JA, Felices M, Yin CC, Reiner SL, Berg LJ. The Tec family tyrosine kinases Itk and Rlk regulate the development of conventional CD8+ T cells. Immunity 2006;25:79–91. [PubMed: 16860759]

Azzam HS, Grinberg A, Lui K, Shen H, Shores EW, Love PE. CD5 expression is developmentally regulated by T cell receptor (TCR) signals and TCR avidity. J Exp Med 1998;188:2301–2311. [PubMed: 9858516]

Bogin Y, Ainey C, Beach D, Yablonski D. SLP-76 mediates and maintains activation of the Tec family kinase ITK via the T cell antigen receptor-induced association between SLP-76 and ITK. Proc Natl Acad Sci U S A 2007;104:6638–6643. [PubMed: 17420479]

Broussard C, Fleischacker C, Horai R, Chetana M, Venegas AM, Sharp LL, Hedrick SM, Fowlkes BJ, Schwartzberg PL. Altered development of CD8+ T cell lineages in mice deficient for the Tec kinases Itk and Rlk. Immunity 2006;25:93–104. [PubMed: 16860760]

Bubeck Wardenburg J, Pappu R, Bu JY, Mayer B, Chernoff J, Straus D, Chan AC. Regulation of PAK activation and the T cell cytoskeleton by the linker protein SLP-76. Immunity 1998;9:607–616. [PubMed: 9846482]

Bunnell SC, Diehn M, Yaffe MB, Findell PR, Cantley LC, Berg LJ. Biochemical interactions integrating Itk with the T cell receptor-initiated signaling cascade. Journal of Biological Chemistry 2000;275:2219–2230. [PubMed: 10636929]

Cante-Barrett K, Gallo EM, Winslow MM, Crabtree GR. Thymocyte negative selection is mediated by protein kinase C- and Ca2+-dependent transcriptional induction of bim [corrected]. J Immunol 2006;176:2299–2306. [PubMed: 16455986]

Chiu CW, Dalton M, Ishiai M, Kurosaki T, Chan AC. BLNK: molecular scaffolding through 'cis'-mediated organization of signaling proteins. Embo J 2002;21:6461–6472. [PubMed: 12456653]

Cho HJ, Edmondson SG, Miller AD, Sellars M, Alexander ST, Somersan S, Punt JA. Cutting edge: identification of the targets of clonal deletion in an unmanipulated thymus. J Immunol 2003;170:10–13. [PubMed: 12496375]

Clements JL, Yang B, Ross-Barta SE, Eliason SL, Hrstka RF, Williamson RA, Koretzky GA. Requirement for the leukocyte-specific adapter protein SLP-76 for normal T cell development. Science 1998;281:416–419. [PubMed: 9665885]

Costello PS, Walters AE, Mee PJ, Turner M, Reynolds LF, Prisco A, Sarner N, Zamoyska R, Tybulewicz VL. The Rho-family GTP exchange factor Vav is a critical transducer of T cell receptor signals to the calcium, ERK, and NF-kappaB pathways. Proc Natl Acad Sci U S A 1999;96:3035–3040. [PubMed: 10077632]

Crispe IN, Bevan MJ. Expression and functional significance of the J11d marker on mouse thymocytes. J Immunol 1987;138:2013–2018. [PubMed: 2435787]

Cunningham NR, Artim SC, Fornadel CM, Sellars MC, Edmonson SG, Scott G, Albino F, Mathur A, Punt JA. Immature CD4+CD8+ thymocytes and mature T cells regulate Nur77 distinctly in response to TCR stimulation. J Immunol 2006;177:6660–6666. [PubMed: 17082578]

Daniels MA, Teixeiro E, Gill J, Hausmann B, Roubaty D, Holmberg K, Werlen G, Hollander GA, Gascoigne NR, Palmer E. Thymic selection threshold defined by compartmentalization of Ras/MAPK signalling. Nature 2006;444:724–729. [PubMed: 17086201]

Dombroski D, Houghtling RA, Labno CM, Precht P, Takesono A, Caplen NJ, Billadeau DD, Wange RL, Burkhardt JK, Schwartzberg PL. Kinase-independent functions for Itk in TCR-induced regulation of Vav and the actin cytoskeleton. J Immunol 2005;174:1385–1392. [PubMed: 15661896]

Duplay P, Lancki D, Allison JP. Distribution and ontogeny of CD2 expression by murine T cells. J Immunol 1989;142:2998–3005. [PubMed: 2565352]

Fischer KD, Kong YY, Nishina H, Tedford K, Marengere LE, Kozieradzki I, Sasaki T, Starr M, Chan G, Gardener S, et al. Vav is a regulator of cytoskeletal reorganization mediated by the T-cell receptor. Curr Biol 1998;8:554–562. [PubMed: 9601639]

Gadue P, Stein PL. NK T cell precursors exhibit differential cytokine regulation and require Itk for efficient maturation. J Immunol 2002;169:2397–2406. [PubMed: 12193707]

Godfrey DI, Berzins SP. Control points in NKT-cell development. Nat Rev Immunol 2007;7:505–518. [PubMed: 17589542]

Godfrey DI, Kennedy J, Suda T, Zlotnik A. A developmental pathway involving four phenotypically and functionally distinct subsets of CD3-CD4-CD8- triple-negative adult mouse thymocytes defined by CD44 and CD25 expression. J Immunol 1993;150:4244–4252. [PubMed: 8387091]

Haase VH, Glickman JN, Socolovsky M, Jaenisch R. Vascular tumors in livers with targeted inactivation of the von Hippel-Lindau tumor suppressor. Proc Natl Acad Sci U S A 2001;98:1583–1588. [PubMed: 11171994]

Houtman JC, Yamaguchi H, Barda-Saad M, Braiman A, Bowden B, Appella E, Schuck P, Samelson LE. Oligomerization of signaling complexes by the multipoint binding of GRB2 to both LAT and SOS1. Nat Struct Mol Biol 2006;13:798–805. [PubMed: 16906159]

Huang Y, Burkhardt JK. T-cell-receptor-dependent actin regulatory mechanisms. J Cell Sci 2007;120:723–730. [PubMed: 17314246]

Jordan MS, Sadler J, Austin JE, Finkelstein LD, Singer AL, Schwartzberg PL, Koretzky GA. Functional hierarchy of the N-terminal tyrosines of SLP-76. J Immunol 2006;176:2430–2438. [PubMed: 16456002]

Jordan MS, Singer AL, Koretzky GA. Adaptors as central mediators of signal transduction in immune cells. Nat Immunol 2003;4:110–116. [PubMed: 12555096]

Kaye J, Hsu ML, Sauron ME, Jameson SC, Gascoigne NR, Hedrick SM. Selective development of CD4 + T cells in transgenic mice expressing a class II MHC-restricted antigen receptor. Nature 1989;341:746–749. [PubMed: 2571940]

Kishimoto H, Surh CD, Sprent J. Upregulation of surface markers on dying thymocytes. J Exp Med 1995;181:649–655. [PubMed: 7836919]

Krawczyk C, Oliveira-dos-Santos A, Sasaki T, Griffiths E, Ohashi PS, Snapper S, Alt F, Penninger JM. Vav1 controls integrin clustering and MHC/peptide-specific cell adhesion to antigen-presenting cells. Immunity 2002;16:331–343. [PubMed: 11911819]

Kumar L, Pivniouk V, de la Fuente MA, Laouini D, Geha RS. Differential role of SLP-76 domains in T cell development and function. Proc Natl Acad Sci U S A 2002;99:884–889. [PubMed: 11792851]

Labno CM, Lewis CM, You D, Leung DW, Takesono A, Kamberos N, Seth A, Finkelstein LD, Rosen MK, Schwartzberg PL, Burkhardt JK. Itk functions to control actin polymerization at the immune synapse through localized activation of Cdc42 and WASP. Curr Biol 2003;13:1619–1624. [PubMed: 13678593]

Liu KQ, Bunnell SC, Gurniak CB, Berg LJ. T cell receptor-initiated calcium release is uncoupled from capacitative calcium entry in Itk-deficient T cells. J Exp Med 1998;187:1721–1727. [PubMed: 9584150]

Mariathasan S, Zakarian A, Bouchard D, Michie AM, Zuniga-Pflucker JC, Ohashi PS. Duration and strength of extracellular signal-regulated kinase signals are altered during positive versus negative thymocyte selection. J Immunol 2001;167:4966–4973. [PubMed: 11673503]

McGargill MA, Hogquist KA. Antigen-induced coreceptor down-regulation on thymocytes is not a result of apoptosis. J Immunol 1999;162:1237–1245. [PubMed: 9973375]

McNeil LK, Starr TK, Hogquist KA. A requirement for sustained ERK signaling during thymocyte positive selection in vivo. Proc Natl Acad Sci U S A 2005;102:13574–13579. [PubMed: 16174747]

Michie AM, Zuniga-Pflucker JC. Regulation of thymocyte differentiation: pre-TCR signals and beta-selection. Semin Immunol 2002;14:311–323. [PubMed: 12220932]

Miosge L, Zamoyska R. Signalling in T-cell development: is it all location, location, location? Curr Opin Immunol 2007;19:194–199. [PubMed: 17306519]

Musci MA, Motto DG, Ross SE, Fang N, Koretzky GA. Three domains of SLP-76 are required for its optimal function in a T cell line. Journal of Immunology 1997;159:1639–1647.

Myung PS, Derimanov G, Jordan MS, Punt JA, Liu QH, Judd BA, Sigmund CD, Freedman BC, Koretzky GA. Differential requirement for SLP-76 domains in T cell development and function. Immunity 2001;15:1011–1026. [PubMed: 11754821]

Neilson JR, Winslow MM, Hur EM, Crabtree GR. Calcineurin B1 is essential for positive but not negative selection during thymocyte development. Immunity 2004;20:255–266. [PubMed: 15030770]

Peterson DO, Kriz KG, Marich JE, Toohey MG. Sequence organization and molecular cloning of mouse mammary tumor virus DNA endogenous to C57BL/6 mice. J Virol 1985;54:525–531. [PubMed: 2985815]

Pivniouk V, Tsitsikov E, Swinton P, Rathbun G, Alt FW, Geha RS. Impaired viability and profound block in thymocyte development in mice lacking the adaptor protein SLP-76. Cell 1998;94:229–238. [PubMed: 9695951]

Pletneva EV, Sundd M, Fulton DB, Andreotti AH. Molecular details of Itk activation by prolyl isomerization and phospholigand binding: the NMR structure of the Itk SH2 domain bound to a phosphopeptide. J Mol Biol 2006;357:550–561. [PubMed: 16436281]

Raab M, da Silva AJ, Findell PR, Rudd CE. Regulation of Vav-SLP-76 binding by ZAP-70 and its relevance to TCR zeta/CD3 induction of interleukin-2. Immunity 1997;6:155–164. [PubMed: 9047237]

Reynolds LF, Smyth LA, Norton T, Freshney N, Downward J, Kioussis D, Tybulewicz VL. Vav1 transduces T cell receptor signals to the activation of phospholipase C-gamma1 via phosphoinositide

3-kinase-dependent and -independent pathways. J Exp Med 2002;195:1103–1114. [PubMed: 11994416]

Richie LI, Ebert PJ, Wu LC, Krummel MF, Owen JJ, Davis MM. Imaging synapse formation during thymocyte selection: inability of CD3zeta to form a stable central accumulation during negative selection. Immunity 2002;16:595–606. [PubMed: 11970882]

Salinas J, Zerial M, Filipski J, Crepin M, Bernardi G. Nonrandom distribution of MMTV proviral sequences in the mouse genome. Nucleic Acids Res 1987;15:3009–3022. [PubMed: 3031617]

Schaeffer EM, Broussard C, Debnath J, Anderson S, McVicar DW, Schwartzberg PL. Tec family kinases modulate thresholds for thymocyte development and selection. J Exp Med 2000;192:987–1000. [PubMed: 11015440]

Schaeffer EM, Debnath J, Yap G, McVicar D, Liao XC, Littman DR, Sher A, Varmus HE, Lenardo MJ, Schwartzberg PL. Requirement for Tec kinases Rlk and Itk in T cell receptor signaling and immunity. Science 1999;284:638–641. [PubMed: 10213685]

Su YW, Zhang Y, Schweikert J, Koretzky GA, Reth M, Wienands J. Interaction of SLP adaptors with the SH2 domain of Tec family kinases. European Journal of Immunology 1999;29:3702–3711. [PubMed: 10556826]

Takahama Y, Shores EW, Singer A. Negative selection of precursor thymocytes before their differentiation into CD4+CD8+ cells. Science 1992;258:653–656. [PubMed: 1357752]

Tarakhovsky A, Kanner SB, Hombach J, Ledbetter JA, Muller W, Killeen N, Rajewsky K. A role for CD5 in TCR-mediated signal transduction and thymocyte selection. Science 1995;269:535–537. [PubMed: 7542801]

Teh HS, Kishi H, Scott B, Von Boehmer H. Deletion of autospecific T cells in T cell receptor (TCR) transgenic mice spares cells with normal TCR levels and low levels of CD8 molecules. J Exp Med 1989;169:795–806. [PubMed: 2494291]

Turner M, Mee PJ, Walters AE, Quinn ME, Mellor AL, Zamoyska R, Tybulewicz VL. A requirement for the Rho-family GTP exchange factor Vav in positive and negative selection of thymocytes. Immunity 1997;7:451–460. [PubMed: 9354466]

Watanabe H, Ohtsuka K, Kimura M, Ikarashi Y, Ohmori K, Kusumi A, Ohteki T, Seki S, Abo T. Details of an isolation method for hepatic lymphocytes in mice. J Immunol Methods 1992;146:145–154. [PubMed: 1531671]

Wu J, Motto DG, Koretzky GA, Weiss A. Vav and SLP-76 interact and functionally cooperate in IL-2 gene activation. Immunity 1996;4:593–602. [PubMed: 8673706]

Wu JN, Gheith S, Bezman NA, Liu QH, Fostel LV, Swanson AM, Freedman BD, Koretzky GA, Peterson EJ. Adhesion- and degranulation-promoting adapter protein is required for efficient thymocyte development and selection. J Immunol 2006;176:6681–6689. [PubMed: 16709827]

Yablonski D, Kadlecek T, Weiss A. Identification of a phospholipase C-gamma1 (PLC-gamma1) SH3 domain-binding site in SLP-76 required for T-cell receptor-mediated activation of PLC-gamma1 and NFAT. Molecular & Cellular Biology 2001;21:4208–4218. [PubMed: 11390650]

Zhang W, Sommers CL, Burshtyn DN, Stebbins CC, DeJarnette JB, Trible RP, Grinberg A, Tsay HC, Jacobs HM, Kessler CM, et al. Essential role of LAT in T cell development. Immunity 1999;10:323–332. [PubMed: 10204488]
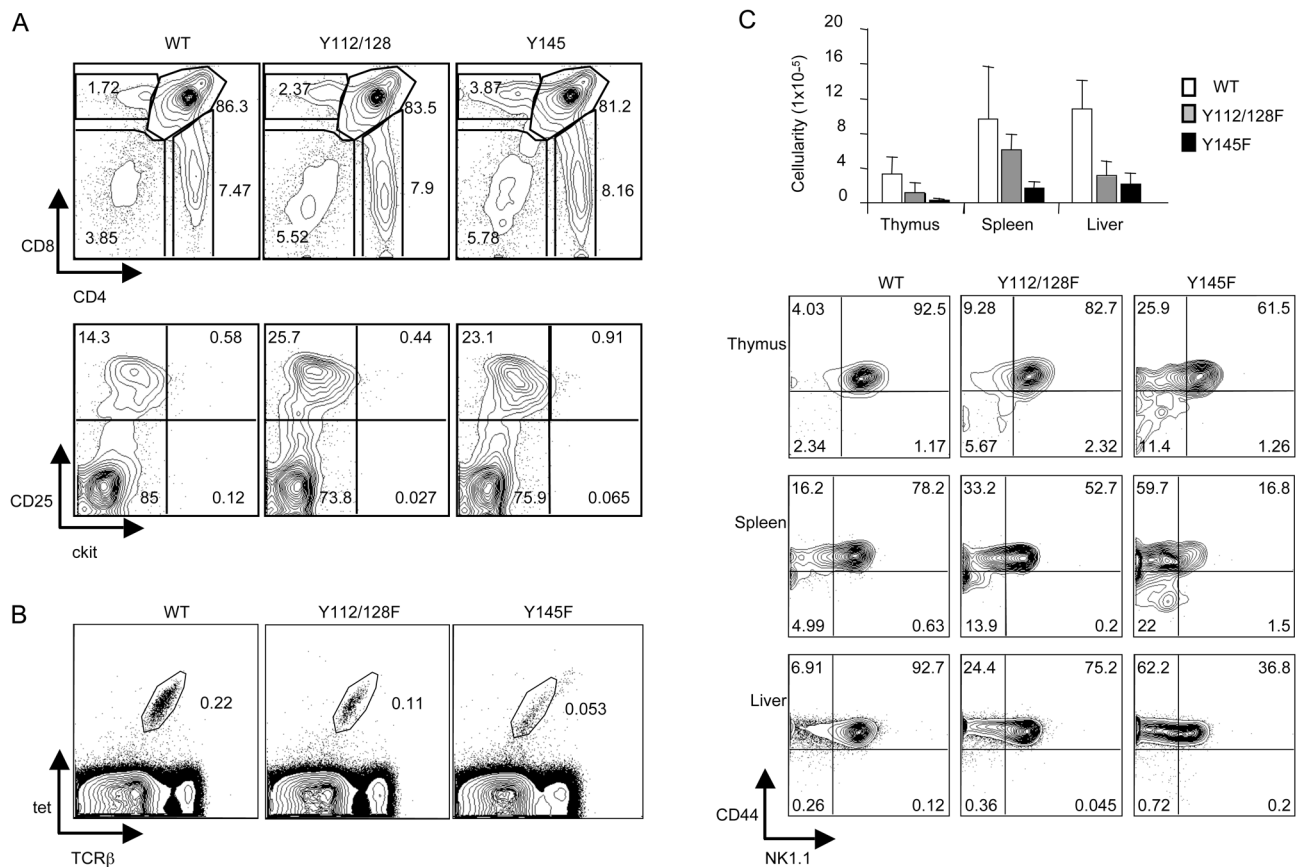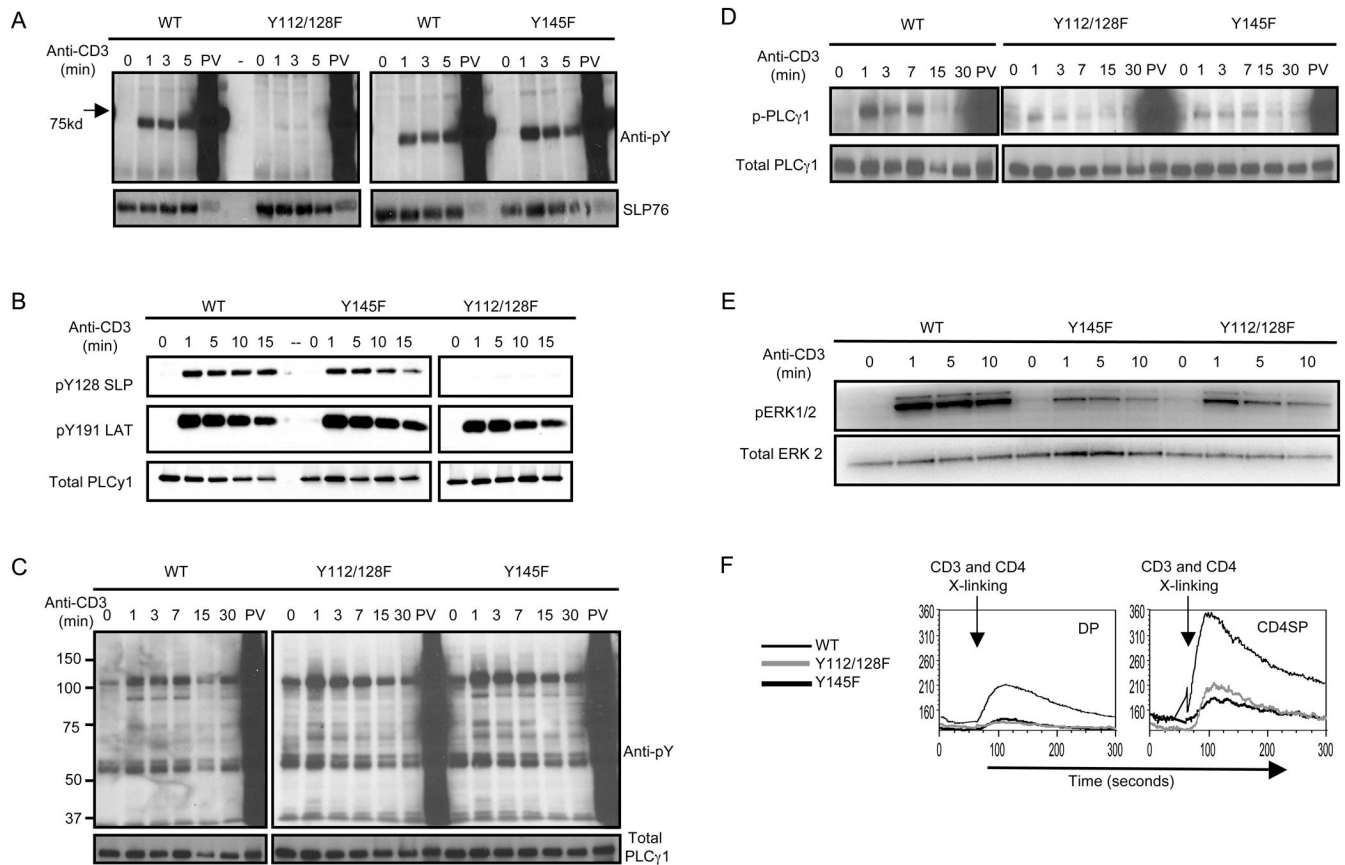
**Figure 1.**
Altered thymic development in SLP76 KI mice. A. Thymocytes from WT, Y145F, and Y112/128F mice were stained with anti-CD4 and anti-CD8 antibodies to determine DN, DP, and SP populations. Contour plots (top row) are representative of 25 mice. DN1–DN4 populations were determined by analyzing CD25 versus ckit expression on thy1.2$^+$ lineage$^-$ (lineage$^-$ gate consisted of antibodies directed to CD8, B220, DX5, NK1.1, TCRγδ, Mac1, and Gr1) thymocytes (n=5). B. Thymic NKT cells were defined as PBS57–CD1d tetramer (tet)$^+$TCRβ$^+$ cells (n=4). C. The absolute number (avg ± SD) of NKT cells from the thymus, spleen, and liver was calculated using the total live cell number of each organ and the percent of tet$^+$TCRβ$^+$ cells (n=4). A student's t-test was used to determine significance. Comparison of WT versus Y112/128F for the thymus, spleen, and liver respectively is as follows: p=0.067, p=0.25, and p=0.002. WT versus Y145F for these organs is as follows: p=0.01, p=0.02 and p=0.0008. Contour plots show the CD44 versus NK1.1 on thymocytes, splenocytes, and liver tet$^+$TCRβ$^+$ cells (n=4).
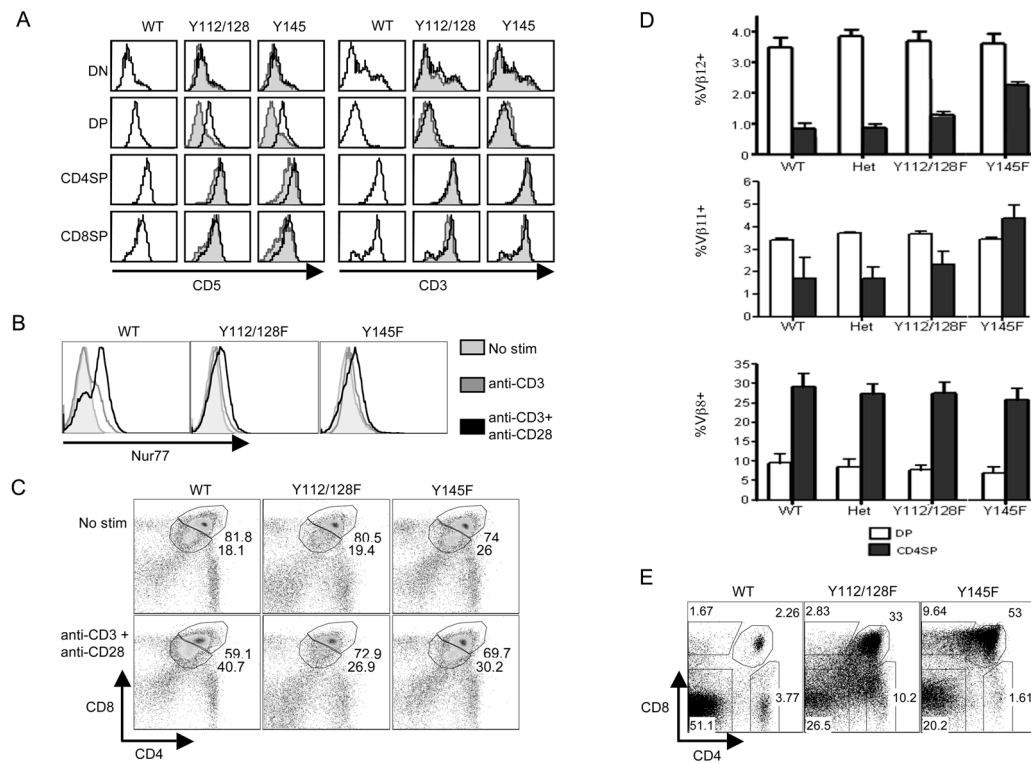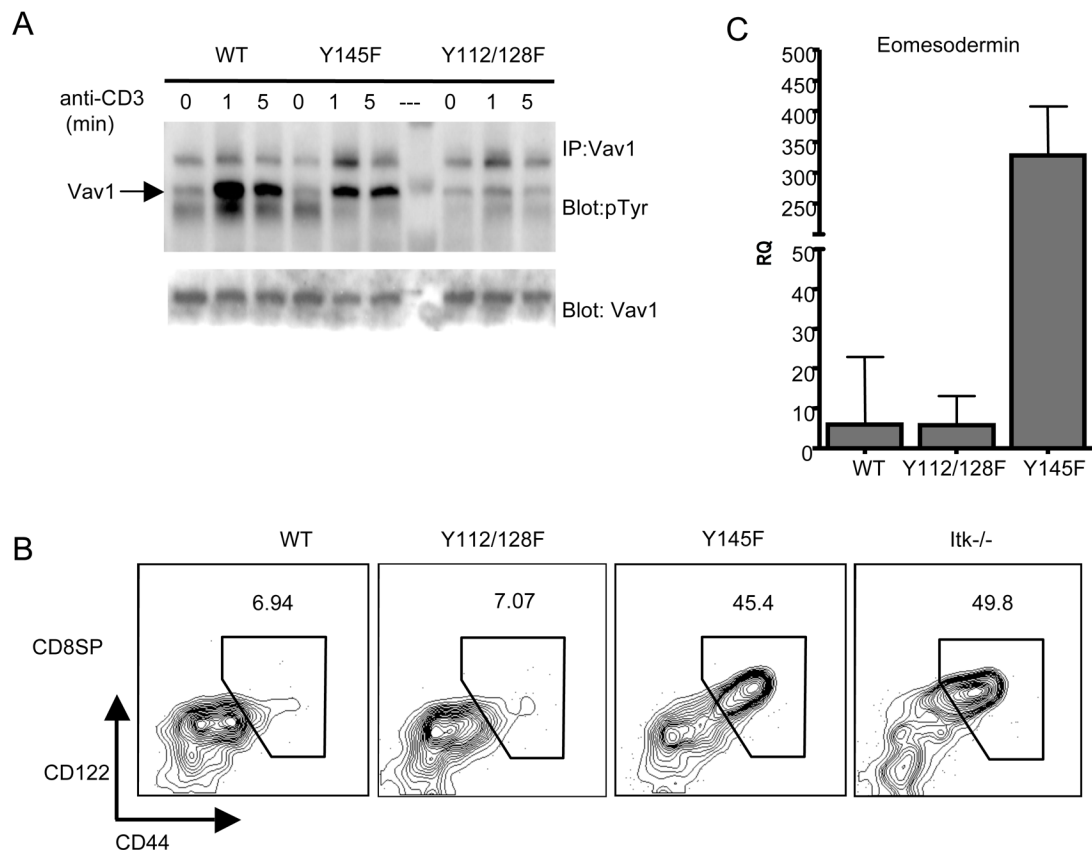
**Figure 2.**
Thymocyte selection in SLP76 KI mice is altered. A. CD5 and CD3 expression is shown on DN, DP, CD4SP and CD8SP thymocytes (n>10). KI mice are represented by the shaded histogram. B. Nur77 expression was measure by flow cytometry on DP thymocytes cultured with anti-CD3, anti-CD3+anti-CD28, or no stimuli for 2 h (n=6–7). C. DP dulling was measured on thymocytes cultured for 5 h. Dot-plots show the percent of DP$^{hi}$ and DP$^{low}$ cells within the DP population (n=5). D. DP and CD4SP thymocytes from WT, KI, and Y112/128F heterozygous mice expressing MHC$^{d}$ were evaluated for expression of Vβ12, 11, and 8. The percent of these Vβ chains among DP and CD4SP populations is shown. The percent of CD4SP Vβ12$^{+}$ and Vβ11$^{+}$ cells in KI mice are statistically significantly different from the percent present in Y112/128F heterzygotes (n=5–10 mice per genotype). E. Thymi from male HY TCR transgenic mice were stained with antibodies to CD4 and CD8. Histograms shows staining with the HY clonotypic antibody T3.70 on DP cells (n=2–6 mice per group).

A



B



C
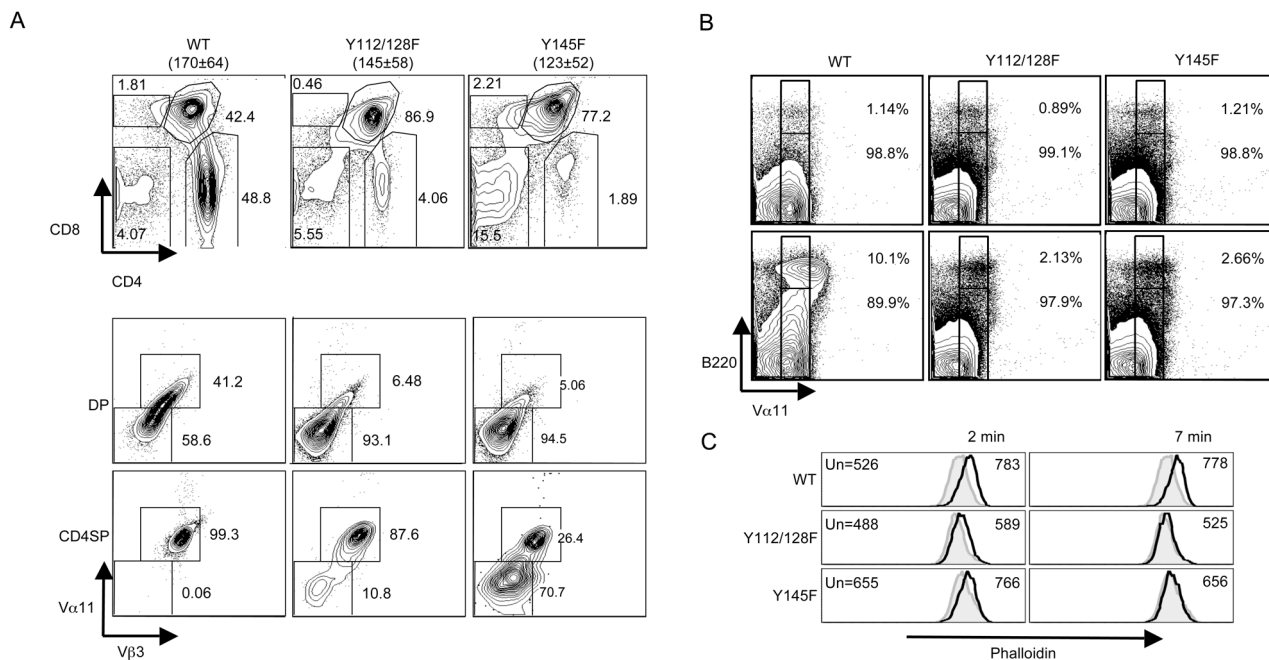


**Figure 3.**
Positive selection and conjugate formation is defective in KI mice. A. The top contour plots show the CD4 versus CD8 profile of total thymocytes from WT, Y112/128F, and Y145F AND TCR transgenic mice (n=4–9). DP and CD4SP populations were evaluated for expression of the transgenic receptor Vβ3/Vα11. B. Contour plots show Vα11 versus B220 expression on DP thymocytes stimulated with PCC loaded (bottom) or non-loaded (top) B cells. Numbers represent the percent of cells that form conjugates with B220+ B cells and the percent that do not among a population of thymocytes expressing the same levels of Vα11 (n=3–4 mice per genotype). C. Actin polymerization was measured in CD4SP thymocytes by flow cytometry following TCR stimulation for 0 min (shaded histogram), 2 or 7 min (black line). Numbers represent the mean fluorescence intensity of the unstimulated (Un) or stimulated peaks. Data are representative of 4 experiments.

**Figure 4.**
KI thymocytes have diminished phosphorylation of PLCγ1 and ERK and diminished Ca$^{2+}$ flux in response to TCR stimulation. A, B, C, and E. Thymocytes were stimulated for the indicated times or with PV for 3 min. In A, SLP76 was immunoprecipitated from the lysates; immunoprecipitations were immunoblotted for total tyrosine phosphorylation using 4G10. SLP76 was used as a loading control (n=3). In B, C and E, thymocyte lysates were immunoblotted with the indicated antibodies. Antibodies against total PLCγ1 or ERK2 were used as loading controls (n=5). D. Ca$^{2+}$ flux was measured from WT (thin black line), Y112/128F (thick grey line), or Y14F (thick black line) from DP or CD4SP gated thymocytes by flow cytometry following CD3 and CD4 cross-linking (n=6).

**Figure 5.**
Thymocytes from Y112/128F and Y145F mice have distinctive signaling defects. A. Vav1
was immunoprecipitated from thymocyte lysates, and phosphorylation of Vav1 was
determined by immunoblotting with anti-phospho-tyrosine antibody (4G10). Total Vav1 levels
were used as a loading control (n=3). B. Thymocytes from WT, Y112/128F, Y145F and
Itk$^{-/-}$ mice were stained with anti-CD4 and anti-CD8 antibodies. CD8SP cells were evaluated
for expression of CD44 and CD122 (n>7). C. CD8SP, CD69$^{+}$ and CD4SP, CD69$^{+}$ thymocytes
were purified by flow cytometry. cDNA from sorted cells was generated and used to determine
the relative expression of eomesodermin in each sorted population as compared to the
expression found in WT CD4SP CD69$^{+}$ thymocytes (n=2).
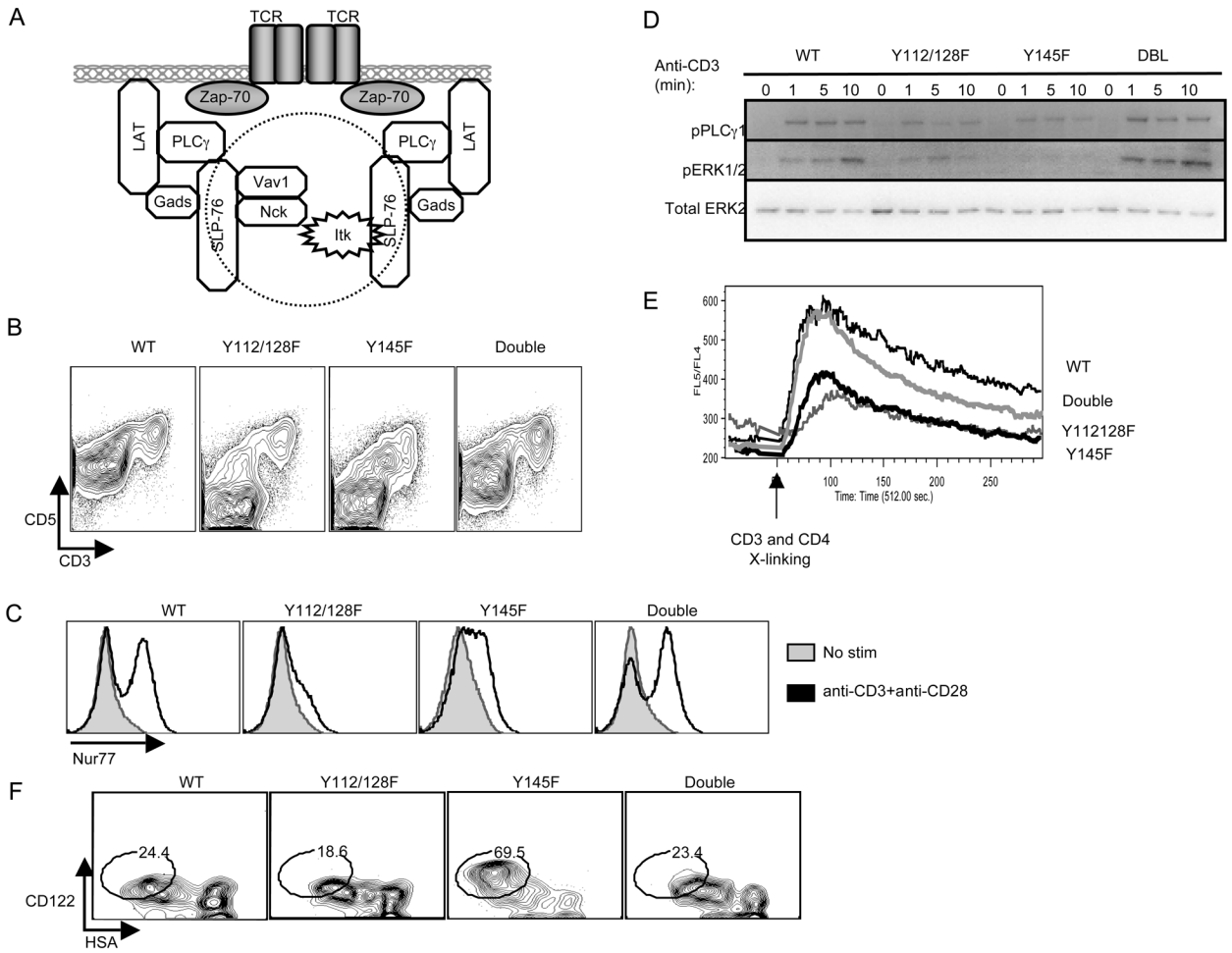
**Figure 6.**
SLP76 KI mutants can complement one another *in trans*. A. Schematic of SLP76 mutants and complex formation. B. Expression of CD3 versus CD5 on total thymocytes from WT, Y112/128F, Y145F, and Double mutant mice (n=4). C. Histograms show the expression of Nur77 on DP thymocytes following 2h of stimulation with media alone (shaded histograms) or anti-CD3+anti-CD28 antibodies (thick black line) (n=3). D. Lysates from anti-CD3 stimulated WT, Y112/128F, Y145F, and Double mutant thymocytes were analyzed by Western blot for phosphorylation of PLCγ1 and ERK (n=3). E. $Ca^{2+}$ flux was induced by crosslinking CD3 and CD4. The tracings represent the relative amount of $Ca^{2+}$ released in CD4SP thymocytes from WT (thin black line), the Double mutant (thick grey line), or Y112/1284F (thick grey line) and Y145F (thick black line) mice (n=4). F. Contour plots show HSA versus CD122 expression on CD8SP thymocytes.